Progress in Cardiovascular Diseases 55 (2012) 234–243.e2
www.onlinepcd.com

Right ventricular assist device in end-stage pulmonary arterial hypertension: insights from a computational model of the cardiovascular system

Lynn Punnoose[a,*], Daniel Burkhoff[b], Stuart Rich[c], Evelyn M. Horn[a]

[a]*Division of Cardiology, Weill Cornell Medical College, New York, NY*
[b]*Division of Cardiology, Columbia University College of Physicians and Surgeons, New York, NY*
[c]*University of Chicago, Chicago, IL*

Abstract

Background: The high mortality rate of pulmonary arterial hypertension (PAH) mainly relates to progressive right ventricular (RV) failure. With limited efficacy of medical therapies, mechanical circulatory support for the RV has been considered. However, there is lack of understanding of the hemodynamic effects of mechanical support in this setting.
Methods: We modeled the cardiovascular system, simulated cases of PAH and RV dysfunction and assessed the theoretical effects of a continuous flow micro-pump as an RV assist device (RVAD). RVAD inflow was sourced either from the RV or RA and outflow was to the pulmonary artery. RVAD support was set at various flow rates and additional simulations were carried out in the presence of atrial septostomy (ASD) and tricuspid regurgitation (TR).
Results: RVAD support increased LV filling, thus improving cardiac output and arterial pressure, unloading the RA and RV, while raising pulmonary arterial and capillary pressures in an RVAD flow-dependent manner. These effects diminished with increasing disease severity. The presence of TR did not significantly impact the hemodynamic effects of RVAD support. ASD reduced the efficacy of RVAD support, since right-to-left shunting decreased and ultimately reversed with increasing RVAD support due to the progressive drop in RA pressure.
Conclusions: The results of this theoretical analysis suggest that RVAD support can effectively increase cardiac output and decreases RA pressure with the consequence of increasing pulmonary artery and capillary pressures. Especially in advanced PAH, low RVAD flow rates may mitigate these potentially detrimental effects while effectively increasing systemic hemodynamics. (Prog Cardiovasc Dis 2012;55:234-243.e2)
© 2012 Elsevier Inc. All rights reserved.

Keywords: Pulmonary arterial hypertension; Right ventricular failure; Mechanical circulatory support

Multiple medical modalities have been introduced in the last decade for the treatment of World Health Organization (WHO) Group I pulmonary artery hypertension (PAH), including intravenous prostacyclin,[1,2] subcutaneous treprostinil,[3] inhaled iloprost,[4] inhaled treprostinil,[5] oral endothelin receptor antagonists[6] and oral phosphodiesterase inhibitors.[7] Nevertheless and despite these successes, mortality still ranges between 20% and 40% three years after diagnosis[8,9] predominantly due to progressive right ventricular (RV) failure.

Whereas the gradual onset of RV hypertrophy (RVH) in congenital heart disease allows for a robust and long term compensatory hypertrophic response, in most other WHO Group I PAH patients, this initial well compensated RVH more rapidly progresses to impaired RV contractility,[8] RV chamber dilatation and leftward shift of the interventricular

Statement of Conflict of Interest: See page 242.

* Address reprint requests to Lynn Punnoose MD, 520 East 70th Street, Starr 4, New York, NY 10021.
E-mail address: punnoosl@alum.mit.edu (L. Punnoose).

0033-0620/$ – see front matter © 2012 Elsevier Inc. All rights reserved.
http://dx.doi.org/10.1016/j.pcad.2012.07.008

Abbreviations and Acronyms

ASD = atrial septal defect

CGS = cardiogenic shock

CO = cardiac output

CVP = central venous pressure

ECMO = extracorporeal membrane oxygenation

LA = left atrium

LV = left ventricle

MCSD = mechanical circulatory support devices

PA = pulmonary artery

PAH = pulmonary arterial hypertension

PCWP = pulmonary capillary wedge pressure

PV = pressure-volume

PVR = pulmonary vascular resistance

RA = right atrium

RV = right ventricle

RVAD = right ventricular assist device

RVH = right ventricular hypertrophy

VAD = ventricular assist device

septum.[10] This then leads to under filling of the left ventricle (LV), systemic hypotension and a lethal combination of RV ischemia, acidosis, pulmonary hypertension crisis and ultimately, cardiogenic shock.

With the advent of successful mechanical circulatory support devices (MCSD) for the failing LV and their more recent use for supporting the RV in conditions of biventricular heart failure in some of myocarditis, post-cardiotomy, post left ventricular assist device (LVAD) and heart transplant patients,[10,11] the use of MCSD for cardiogenic shock associated with PAH and isolated RV failure is being considered. However, the hemodynamic effects of RV support in the setting of severely elevated pulmonary vascular resistance (PVR), in the absence of concomitant mechanical support of the left ventricle or the use of extracorporeal membrane oxygenation (ECMO), have not been delineated. In the absence of clinical data and the unlikelihood of such data becoming available in the short term, it is reasonable and appropriate to turn to computer simulations to provide insights into the potential benefits and hazards of isolated right ventricular support in PAH. This topic is timely due to the availability of new, small mechanical circulatory assist devices with low flow capabilities. The Synergy micropump system[12–14] is one such pump that can be configured for right-sided support (Fig 1) and has been proposed for use in this specific patient population.

Therefore, the purpose of this study was to employ a previously validated computational model of the circulatory system to simulate varying degrees of PAH disease severity and to predict the hemodynamic effects of varying degrees of right ventricular support. Simulations were also performed in the presence of a simulated atrial septostomy, a form of therapy employed in some centers for medically refractory PAH.[15]

Methods

Ventricular and atrial contractile properties were modeled as time-varying elastances and the systemic and pulmonary vascular beds were modeled by series of resistance and capacitance elements as detailed previously[16] and summarized in the Appendix. Right-sided mechanical circulatory support was modeled by incorporating a pump with the pressure-flow characteristics of the Synergy™ continuous flow micro-pump (CircuLite Inc, Saddle Brook, NJ), also detailed in the Appendix. RVAD blood flow could be sourced from either the right atrium or from the right ventricle and was ejected into the proximal pulmonary artery. Atrial septostomy was modeled by incorporating a blood flow path between the right and left atria with a resistance determined by the equations governing flow through an orifice. Five sets of model parameter values were established to simulate hemodynamic conditions of varying degrees of PAH and RV dysfunction, yielding overall conditions ranging from mild right-sided failure to severe right-sided failure with cardiogenic shock (CGS). The hemodynamic characteristics of these patients were determined from a review of the literature[17,18] and are summarized in Table 1. Parameter values of the model were adjusted by a custom designed algorithm to fit the hemodynamic conditions for each of these conditions. Parameters that were varied included those that determine right and left ventricular chamber systolic and diastolic properties (E_{es} and α, respectively), vascular resistance (Ra and Rc), vascular compliance (C) for both systemic and pulmonary beds and stressed

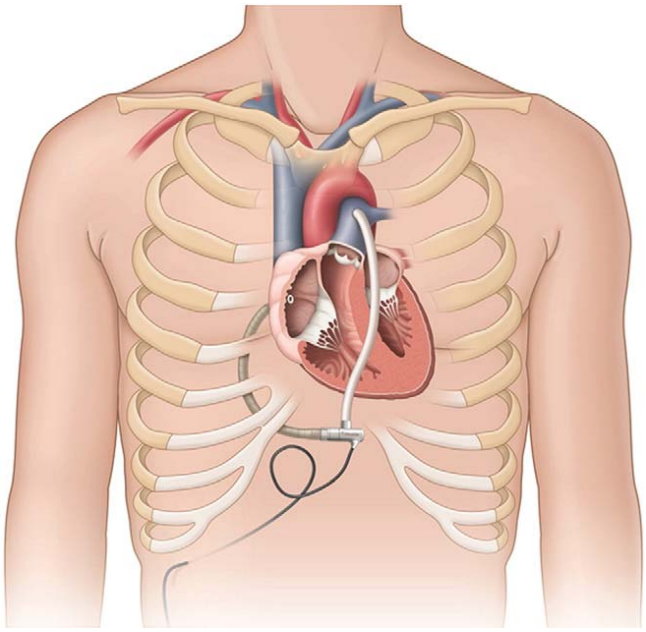

Fig 1. Schematic of mechanical circulatory support device, with inflow cannula in the RA and outflow in the PA.

Table 1
Sample patient hemodynamics and chamber volumes for simulation.

	Severity of pulmonary hypertension				
Parameter	Normal	Mild	Moderate	Severe	CGS
HR (bpm)	60	60	75	85	95
LVEF (%)	55	55	55	55	55
CO (L/min)	5	4.75	4.4	3.5	2.5
CVP (mmHg)	7	12	18	25	25
PASP (mmHg)	20	60	80	100	80
PADP (mmHg)	12	30	35	50	44
mPAP (mmHg)	15	40	50	67	56
PCWP (mmHg)	8	10	10	8	8
Ao-S (mmHg)	130	130	110	90	75
Ao-D (mmHg)	70	70	60	60	52
MAP (mmHg)	87	87	76	70	61
RA volume (mL)	70	100	140	160	160
RV volume (mL)	150	150	200	250	250
LA volume (mL)	70	70	70	70	70
Stressed volume (mL)	1200	1980	2420	2560	2500

AO-D, diastolic aortic pressure; Ao-S, systolic aortic pressure; CGS, cardiogenic shock; CO, cardiac output; CVP, central venous pressure; HR, heart rate; LA, left atrium; LVEF, left ventricular ejection fraction; MAP, mean arterial pressure; mPAP, mean pulmonary arterial pressure; PADP, pulmonary artery diastolic pressure; PASP, pulmonary artery systolic pressure; PCWP, pulmonary capillary wedge pressure; RA, right atrium; RV, right ventricle.

blood volume (which correlates with patient overall fluid status). Values of key parameters are summarized in Table 2 and detailed further in Appendix Table A1.

Aortic, pulmonary arterial, ventricular and atrial pressure waveforms, as well as RV and LV pressure volume (PV) loops, were constructed for each disease state. The effects of RVAD flow rate on these waveforms, as well as on aortic and pulmonary arterial pressures, central venous pressure (CVP), pulmonary capillary wedge pressures (PCWP) and left-sided cardiac output (CO) were determined. Total blood flow to the pulmonary artery was the sum of VAD flow plus residual flow generated directly by the RV. Additional calculations were carried out for simulated patients with a 6 mm diameter atrial septostomy, with and without an RVAD.

Results

Review of the literature indicates that with increasing disease severity, there is progressive RV chamber dilation (corresponding with decreasing diastolic stiffness constant, α)[17] and hypertrophy with increases in contractile strength (corresponding with increased E_{es}).[10] RA and PA pressures rise, except in severe end-stage disease with CGS where the RV fails (E_{es} decreases) and is unable to generate higher PA pressures (Tables 1 and 2). On the other hand, with chronic LV underfilling, mean arterial pressures and CO decline. The reduction in LV chamber size appears to be due to structural changes in the LV and shifts of the interventricular septum that result in chamber stiffening (reflected in the increase in the left ventricular diastolic stiffness coefficient, α). Also note that in order to appropriately simulate these cases, stressed blood volumes increased with disease

Table 2
Values of model parameters determined to simulate patients with hemodynamic characteristics with different severities of PAH as summarized in Table 1.

	Severity of pulmonary arterial hypertension				
Parameter	Normal	Mild	Moderate	Severe	CGS
Heart rate (bpm)	60	60	75	85	95
AV delay	160	160	160	160	160
Stressed blood					
Volume (mL)	1200	1980	2420	2560	2500
Systemic circulation					
R_c (mmHg.s/mL)	0.02	0.02	0.02	0.02	0.02
C_a (mL/mmHg)	2.2	2.2	1.3	2.7	1.3
R_a (mmHg.s/mL)	0.92	0.91	0.75	0.73	0.80
Pulmonary circulation					
R_c (mmHg.s/mL)	0.02	0.02	0.10	0.11	0.13
C_a (mL/mmHg)	13	13	13	1.5	1.5
R_a (mmHg.s/mL)	0.03	0.34	0.43	0.85	1.00
Left ventricle					
E_{es} (mmHg/mL)	1.8	1.5	2.1	2.5	4.0
α (mL^{-1})	0.023	0.026	0.035	0.049	0.081
Right ventricle					
E_{es} (mmHg/mL)	0.35	0.61	0.52	0.43	0.32
α (mL^{-1})	0.023	0.020	0.020	0.017	0.017
Left atrium					
E_{es} (mmHg/mL)	0.42	0.44	0.44	0.42	0.42
α (mL^{-1})	0.050	0.050	0.050	0.050	0.050
Right atrium					
E_{es} (mmHg/mL)	0.41	0.31	0.24	0.22	0.22
α (mL^{-1})	0.049	0.037	0.028	0.026	0.026

α, diastolic stiffness coefficient; Ca, arterial capacitance; Ees, end-systolic elastance; Rc, proximal resistance; Ra, arterial resistance.

severity (Table 2) suggesting, consistent with clinical experience, that these patients become increasingly volume overloaded as their disease progresses.

RVADs could be configured to draw blood from either the RA or RV. Fig 2A summarizes the hemodynamic effects of these two configurations in the simulated patient with severe PAH. RV sourcing results in a triangular shaped PV loop, with loss of isovolumic contraction and relaxation periods, significant increases in PA diastolic and mean pressures, and slight increases in PA systolic, LA and aortic pressures. When sourced from the RA, the loop shifts only slightly leftward (lower RV filling) and narrows (indicating a decrease in RV stroke volume). Despite the significantly different impact on the RV pressure-volume loop, the impact on RA, pulmonary, left atrial and aortic pressures achieved with the two configurations are very similar (Fig 2B).

The impact of varying RVAD speed on hemodynamic parameters is summarized in Fig 3. First consider total pulmonary blood flow, which is the sum of native RV output and flow from the RVAD (Fig. 3A). As RVAD speed is increased, RVAD flow increases and native RV output decreases due to the simultaneous reduction in RV filling and increase in pulmonary afterload pressure. In this example, total flow increases from the baseline value of ~3.5 L/min to ~4.75 L/min at maximal RVAD speed. As a result of the increased flow, and assuming pulmonary vascular resistance is fixed, there is a progressive increase in diastolic and mean pulmonary pressures, but systolic pressure does not increase substantially (Fig. 3B). Since LV cardiac output equals the total flow through the pulmonary circuit, this means RVAD support increases LV filling (increased PCWP), resulting in increased aortic pressures (Fig. 3C). Two factors contributing to this rise in pulmonary capillary pressure are the increased stressed blood volume (which predominantly resides in the systemic circulation and is shifted to the pulmonary circulation by the RVAD) and the LV diastolic dysfunction discussed above. Finally, as RVAD flow is increased there is a progressive decrease in CVP.

Figs 2 and 3 illustrate the impact of RVAD support in the simulated case of severe PAH defined according to the data in Table 1. There were qualitatively similar effects of RVAD support on right and left ventricular pressure-volume loops at each stage of PAH disease severity. RVAD support shifted the LV pressure-volume loops rightward towards higher end-diastolic volumes (i.e., increased LV filling), with resultant increases in stroke volume and aortic pressures. Right ventricular

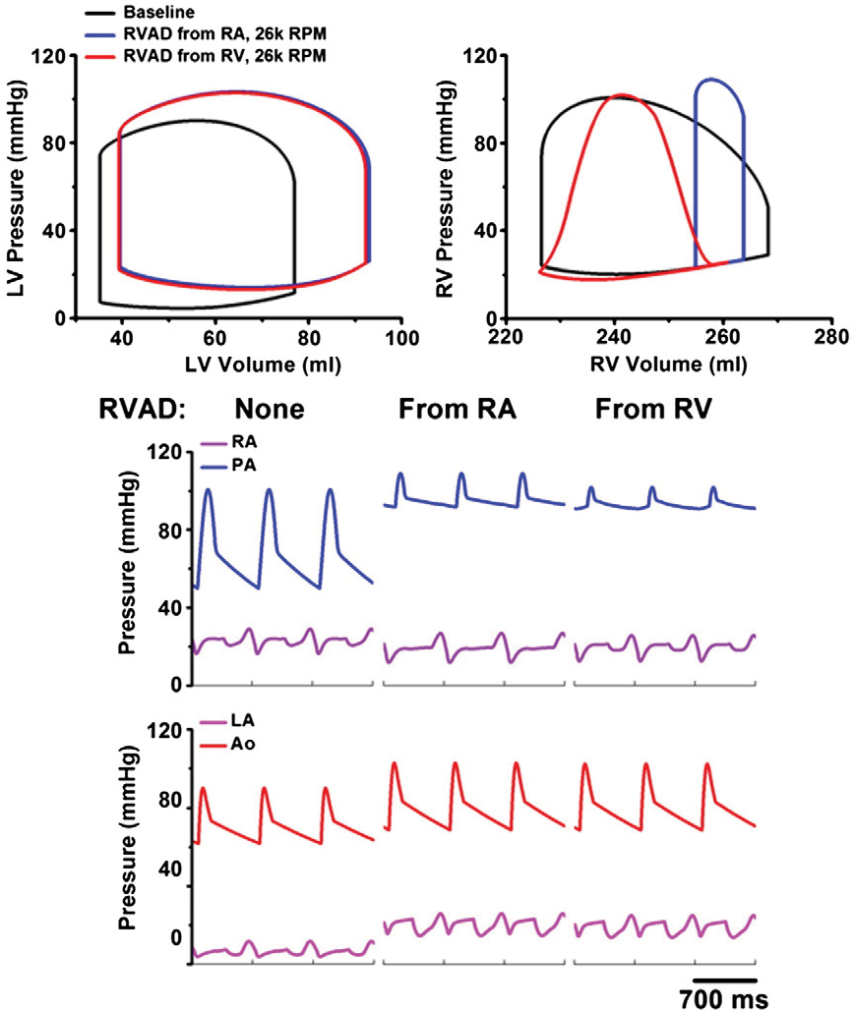

Fig 2. Model simulations of hemodynamic outcomes with RVAD implantation. A, Effects of RVAD implantation on pressure volume loops, with inflow cannula placed in the RA or RV. B, Effects of RVAD implantation on PA, RA, LA and Ao pressures. Abbreviations as per Table 1.

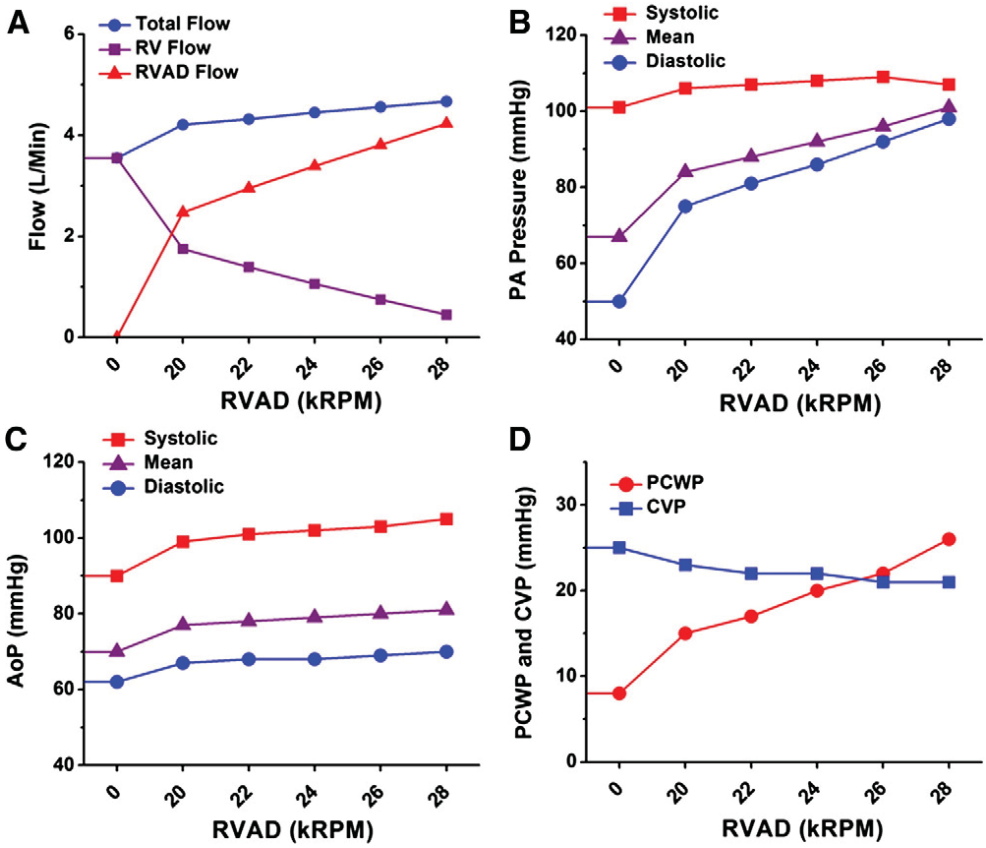

Fig 3. Patient hemodynamics as a function of MCS in severe PAH (RA source). A, Total output compared to RV and device flows. B, PA systolic, diastolic and mean pressures. C, Aortic systolic, diastolic and mean pressures. D, Wedge and central venous pressures.

pressure-volume loops shift leftward (i.e., RV unloading), become narrower with right atrial sourcing, became triangular with right ventricular sourcing and resulted in higher diastolic and mean pulmonary pressures.

However, the effects of RVAD support on hemodynamic parameters varied with PAH disease severity, as summarized in Table 3. Data in this table compare baseline hemodynamic parameters to those simulated with RVAD speed set at 26 krpm with inflow sourced from either the RA or the RV. Central venous pressure decreased by 3–5 mmHg regardless of disease severity or source of inflow. The rise in mean pulmonary artery pressure was similar for RA and RV sourcing of blood and for different levels of PAH disease severity, except in the most extreme case of PAH with cardiogenic shock where the increase was significantly greater with RV sourcing. This was mainly due to the markedly increased pulmonary vascular resistance present in severe PAH (Table 2). The rise in pulmonary capillary wedge pressure was also significantly greater in the end-stage disease states, due to the severity of LV diastolic dysfunction and the increased stressed blood volume.

Tricuspid regurgitation

Most patients with severe pulmonary hypertension have significant tricuspid regurgitation (TR). Therefore, a simulation was performed to investigate the potential implications of TR on the efficacy of right-sided mechanical circulatory support and to address the potential benefits of RVAD implantation in combination with a procedure to eliminate TR. TR was introduced into the model, as detailed in the Appendix, by inclusion of a resistance to backward flow from the right ventricle to the right atrium; the other model parameter values were set at the values determined for severe PAH (Table 2). The value of the resistance was adjusted to simulated moderate-to-severe TR with a regurgitant fraction of 50% which, in this case corresponded to a regurgitant volume of 39 mL/beat. As summarized in Table 4, introduction of TR caused a slight reduction in cardiac output and thus a decrease in pulmonary, pulmonary capillary and aortic pressures, though no significant impact on mean central venous pressure. The overall efficacy of VAD support was not significantly impacted by the presence of TR. When RVAD support was sourced from the right atrium, there was a 0.2 L/min improvement in total cardiac output when TR was removed, which correlated with corresponding increases in pulmonary and systemic pressures. Interestingly, the regurgitant volume *increased* slightly with this RVAD configuration, which was a result of the decrease in right atrial pressure (especially during RV systole which is not reflected in the subtle change in mean pressure shown in the Table) and an increased RV-RA systolic pressure gradient. There was even less of an impact of TR on overall hemodynamics when RVAD support was sourced from the RV and there was also minimal impact of this form of RVAD support on regurgitant volume.

Atrial septostomy with and without RVAD

In the simulated patient with severe PAH, the creation of an atrial septostomy defect (ASD, 6 mm diameter, with resulting

Table 3
Hemodynamic effects of RVAD support set At 26 kRPM, with either RA or RV used as inflow source.

	CVP			mPAP			PCWP			MAP			CO		
PH	Baseline	RVADRA	RVADRV	Baseline	RVADRA	RVADRV	Baseline	RVADRA	RVADRV	Baseline	RVADRA	RVADRV	Baseline	RVADRA	RVADRV
Mild	12	8	9	40	59	55	10	23	20	87	102	101	4.75	5.93	5.75
Moderate	18	13	14	50	73	70	10	24	22	76	86	86	4.4	5.5	5.4
Severe	25	18	18	67	80	79	8	26	25	70	79	79	3.5	4.78	4.74
CGS	25	20	20	56	105	115	8	37	44	61	71	73	2.53	3.63	3.78

right-to-left shunt) resulted in leftward shifting of the RA PV loop towards lower volumes and pressures with a minimal shift in the RV PV loop. In contrast, LA and LV loops shift rightward, reflecting increased filling pressures and end-diastolic volumes (Fig 4). These changes underlie a marked increase in LV CO (Fig 5C) and pulmonary capillary pressure from 8 to 20 mmHg (Fig 5E) and only a modest decrease of 3 mmHg in CVP (Fig 5D). There was no significant change in PA pressures caused by the ASD. Shunt fraction (Qp/Qs) was 0.77 with a 6 mm ASD. Under this condition, with an assumed mixed venous saturation of 74% and pulmonary capillary saturation of 100%, aortic saturation is estimated to be 91% (by the Fick method for a 65 kg, 50 year old female patient with hemoglobin 13.3 g/dL). If the ASD size was increased to 12 mm in diameter, the shunt fraction decreased to only 0.75. Thus, increasing the size of the ASD from 6 to 12 mm did not lead to a marked change in CO or arterial desaturation.

The overall impact of the septostomy on RVAD effects at different speeds in the simulated case of severe PAH is summarized in Fig. 5. The septostomy had no significant impact on RVAD flows (Fig 5B) or mean PA pressures (Fig 5F). Compared to the simulated patient without an ASD, addition of an RVAD at low speeds (≤24 kRPM) did not improve total cardiac output (LV CO, Fig 5C) but, because of the reduction in RA pressure, did decrease shunt flow. Pulmonary capillary pressure was higher at low RVAD flows in the presence of the ASD (Fig 5E). Notably, at higher RVAD flows (i.e., ≥26 kRPM) the drop in RA pressure was sufficient to reverse the flow through the ASD (Fig 5A); compared to the case without an ASD, this lead to lower pulmonary capillary pressures (Fig 5E), but also to lower LV CO (Fig 5C) and no improvement in CVP (Fig 5D). Shunt flow reversal was observed even at low RVAD flows in the patient with moderate disease and an ASD due to earlier reversal of the interatrial pressure gradient.

Discussion

Mechanical support of the failing RV decreases RA pressures and RV stroke work, unloads the RV and increases CO effectively in cases of inferior MI, sepsis and post-cardiotomy RV failure[19] as well as in patients with RV failure after LVAD implantation and orthotopic heart transplantation.[10,11] By contrast, its efficacy in patients with PAH has not been well described. A specific challenge for RVAD use in PAH is how to safely augment flow through a pulmonary vascular bed with significantly elevated resistance and impedance,[20,21] with concerns of damaging the microcirculation leading to pulmonary hemorrhage, as described in one case report.[22] To our knowledge, only two case reports to date detail the use of RVAD in severe PAH and cardiogenic shock.[22,23] In the first,[23] an RVAD was implanted for 56 hours, and it generated higher PA pressures but also rises in CO and aortic pressures[23] without evidence of pulmonary hemorrhage. The second[22] describes suprasystemic pulmonary hypertension immediately after RVAD implantation, with subsequent pulmonary hemorrhage necessitating a switch from RVAD to ECMO for hemodynamic support.

Table 4
Hemodynamic impact of tricuspid regurgitation on RVAD support in different configurations.

	TR	TR Volume mL/beat	RVAD Speed kRPM	RVAD Flow L/min	RV CO L/min	Total CO L/min	CVP mmHg	PAP mmHg	PCP mmHg	AoP mmHg
Baseline	No	0	0	0	3.55	3.55	25	101/50 (67)	8	90/62 (70)
	Yes	37	0	0	3.25	3.25	25	89/45 (60)	6	86/59 (67)
RA-PA VAD	Yes	45	26	3.95	0.44	4.34	22	97/86 (88)	18	101/68 (79)
	No	0	26	3.82	0.77	4.54	21	109/92 (96)	22	103/69 (80)
RV-PA VAD	Yes	39	26	4.2	0.09	4.39	22	92/86 (88)	19	102/69 (79)
	No	0	26	4.19	0.31	4.5	22	102/91 (93)	21	103/69 (80)

TR, tricuspid regurgitation; RA-PA VAD, right atrial-to-pulmonary artery VAD configuration; RV-PA VAD, right ventricular-to-pulmonary artery VAD configuration; RV, right ventricle; CO, cardiac output; CVP, central venous pressure; PAP, pulmonary artery systolic/diastolic (mean) pressure; PCP, pulmonary capillary pressure; AoP, aortic systolic/diastolic (mean) pressure.

The present simulations demonstrate that partial RV circulatory support can significantly augment cardiac output and decrease RA pressures (Table 3) in patients with PAH, RV dysfunction and heart failure. As illustrated by pressure-volume analysis (Fig 2), this is true whether sourcing inflow is from the RA or the RV. RVAD support decreases RV end-diastolic pressures and volumes and increases LV filling, total cardiac output and arterial blood pressure. These hemodynamic improvements are less pronounced in the simulated patients with more severe disease (Table 3), due to progressive increases in pulmonary vascular resistance and fixed RV afterload.

Furthermore, with worsening disease, RVAD support causes significant increases in diastolic and mean pulmonary pressures (Fig 3, Table 3), though not in systolic pulmonary pressure. This is consistent with prior reports of increased PA pressures with RVAD support[20,23] due to increased flows pumping into high resistance vasculatures, particularly with decreasing vascular compliance in more severe disease.[24] However, at present, our model does not incorporate rheological abnormalities of the diseased vasculature.

In addition to higher PA pressures, simulated RVAD flows achieved at 26 kRPM (~3 L/min) also lead to rising pulmonary capillary wedge pressures at every disease severity (Table 3). The effects on pulmonary arterial and venous pressures were markedly more dramatic in the patient with cardiogenic shock, even as CO and RA pressures improved. This result reflects the effect of the increased stressed volumes with increasing degrees of heart failure (Table 1) that are now shifted to a previously underfilled pulmonary circuit and LV. The increased

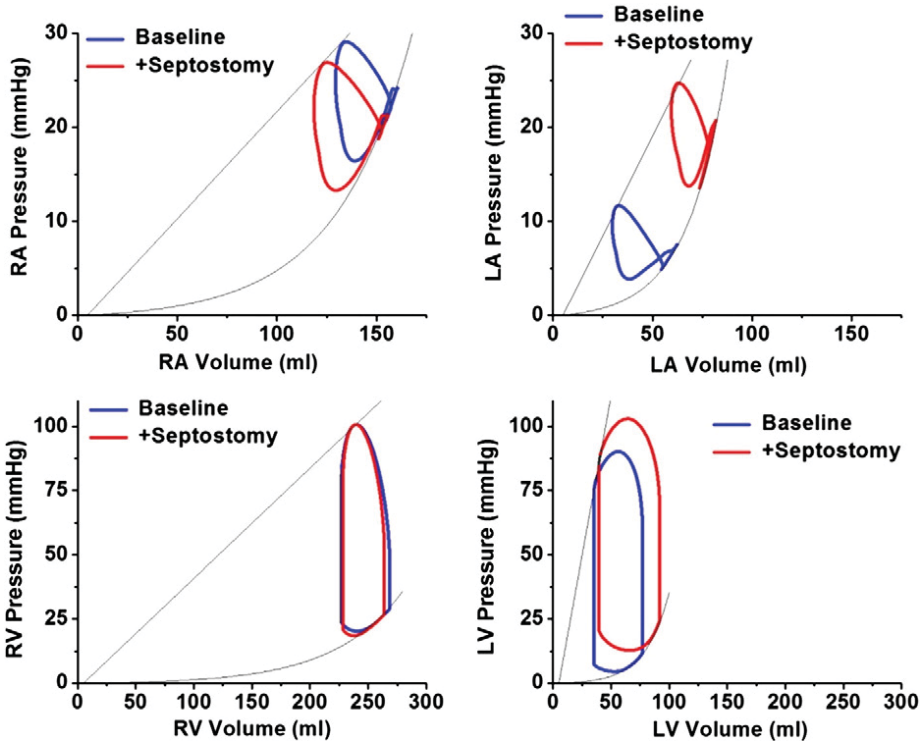

Fig 4. PV loops for each heart chamber generated in severe PAH, with and without atrial septostomy.

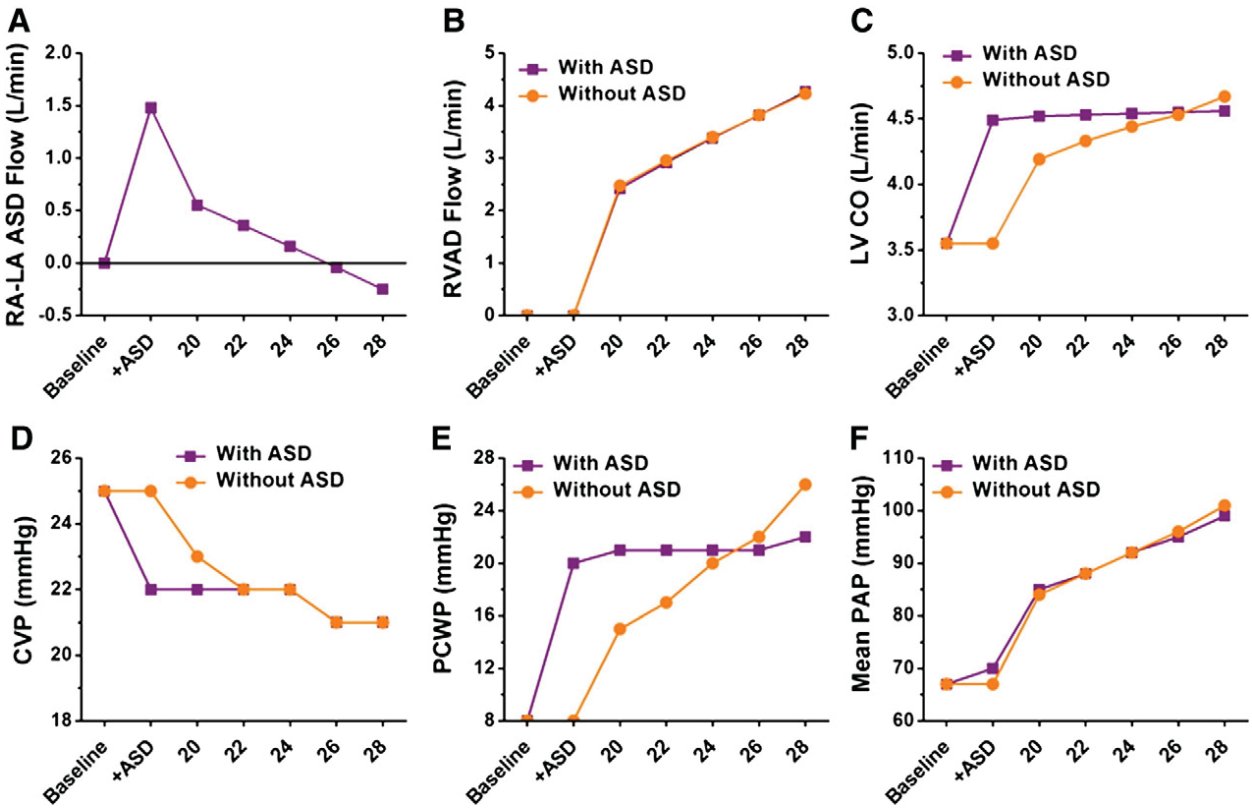

Fig 5. Patient hemodynamics as a function of MCS, with and without atrial septostomy, showing shunt flow (A, positive values indicate right to left shunt), device flows (B), total output (C), CVP (D), PCWP (E) and mPAP (F). Abbreviations as per Table 1.

stressed volumes correlate with clinical practice in that patients with PAH become increasingly volume overloaded due, at a minimum, to renal hypoperfusion and sympathetic activation, which conspire to reduce renal function, the same as in end-stage left-sided heart failure. From a clinical perspective, this picture is also similar to unexpected LV failure following lung transplantation or inhaled nitric oxide[25]: augmented flows to the LV following a decrease in PVR result in significant and abrupt shifts of volume from the peripheral vasculature to the pulmonary circulation. Such abrupt redistribution of volume can result in pulmonary edema, even in the setting of normal LV systolic and diastolic function.[26]

In addition, recent studies in animals[27,28] and humans[29,30] with PAH have provided evidence of LV diastolic dysfunction, manifest as reduced chamber size (i.e., leftward shifted end-diastolic pressure-volume relationship). Indeed, our patient hemodynamic parameter fitting algorithm indicated that with increasing disease severity and progressively lower cardiac outputs, LV diastolic stiffness increased substantially (i.e., higher LV diastolic stiffness coefficient, α, Table 2). Increased LV diastolic stiffness would also be expected to contribute to the risk of increased pulmonary capillary pressure in the setting of large volume shifts from peripheral to pulmonary circulations.

An analysis of the potential impact of tricuspid regurgitation on the effectiveness of RVAD was also performed. The results showed that the presence of TR did not impact significantly on the hemodynamic effectiveness of the RVAD, nor did the RVAD have a significant effect the degree of TR. This appears to be because as disease severity increases, right atrial volume and compliance increase substantially, which has the effect of increasingly dampening the hemodynamic effects of TR. There is, however, one potential *advantage* of the presence of TR with the RVAD when it is used in a configuration that sources blood from the right atrium. Specifically, in severe PAH, the RVAD has the potential to overtake the RV so that there is no output from the native RV. If that happens, there can be stagnation of blood within the RV which has the potential to form intraventricular clots. When significant TR is present, blood continues to flow into and out of the RV with each beat, independent of RVAD speed which, along with standard VAD anticoagulation and antiplatelet therapy, eliminates this possibility. When blood is sourced directly from the RV, this is not a factor. The result of this analysis suggests that there would be no significant benefit of surgically correcting TR at the time of RVAD implantation.

Taken together, our findings would argue for the potential benefits of partial RV support, for starting RVADs at low flows (particularly based on severity of disease) and, importantly, also addressing the higher stressed volumes with diuresis or ultrafiltration if necessary.

Decreasing PVR with vasodilators would also be helpful in the long run; however, patient selection for RVAD support would undoubtedly require failed treatment with vasodilators. It would therefore not be expected that further vasodilation can be achieved in the patients likely to undergo RVAD implantation. On the other hand, preexisting vasodilator therapy should definitely not be withdrawn. Furthermore, it is conceivable that pulmonary capillary pressure could rise even further with additional vasodilation. An earlier simulation of acute and chronic PH showed, consistent with clinical case reports, that higher pulmonary venous pressures and pulmonary edema can result from vasodilation with nitric oxide.[25] As discussed above, this was primarily due to the shift of volume from the systemic to pulmonary vasculature in response to the decreased PVR.

In select patients with advanced PAH and RV dysfunction, atrial septostomy can be performed as a palliative procedure, reducing RA pressures, augmenting flow to the left side, improving systemic output[15] and survival.[31] We hypothesized that an atrial septostomy could both augment CO and mitigate the higher PA pressures produced by the RVAD flows. Indeed, in the patient with severe PAH (PA systolic pressure of 100), baseline RA pressures decreased and CO improved with the addition of an ASD (Fig 5), but without much change in PA pressures. However, the RVAD, by withdrawing blood from either RA or RV, decreased interatrial pressure gradients, diminished the right-to-left shunt flow and then eventually reversed it (Fig 5A). For this reason, adding an RVAD to a patient with an ASD would not appear to produce a further increase in CO (Fig 5C) or decrease in CVP (Fig 5D). In fact, with outright shunt reversal at RVAD speeds of 28 kRPM, LV CO decreases and flow through the pulmonary vascular bed increases due to left-to-right shunting.

Limitations

There are many important limitations inherent in any theoretical simulation and the results should not be considered in detailed quantitative terms. For the current analysis, particular limitations relate to assumptions about the hemodynamic properties of the pulmonary circulation and effects of RVAD implantation. First, the model reflects the acute effects of RVADs, assuming, for example, that PVR, LV diastolic properties and stressed blood volume all remain the same immediately before and after RVAD implantation. However, in the hours or days after RVAD implantation, improved CO and renal flow may promote an augmented diuresis and effectively decrease the stressed blood volumes. Similarly, reduction of sympathetic tone could decrease venous tone and also contribute to decreased stressed volumes. Furthermore, with all of the many changes induced by RVAD support, it is possible that pulmonary properties (and in particular, PVR) may decrease following initiation of support. In such a case, mean PAP may not rise as much as the model predicts. Additionally, the model did not include interventricular interactions with RV unloading. Decreased RV loading will normalize septal motion, improve LV diastolic filling[30] and thereby decrease the effect of stressed volumes; the immediate rise in pulmonary capillary pressure would be reduced over time.

Conclusions

Heart failure in the setting of advanced PAH and RV dysfunction represents a difficult therapeutic challenge. Our hemodynamic model demonstrates that partial circulatory support of the RV can effectively augment CO and decrease RA pressures, but at the expense of RVAD flow-dependent increases in mean PA pressure and pulmonary capillary pressure. These effects were particularly prominent in our simulation of the most advanced and decompensated right heart failure simulation. Thus, the results suggest that low RVAD flows, especially early after initiation of support, minimize these potential adverse effects related to both the added stressed volume on the previously under-filled LV and of the high blood flows through a pulmonary bed with high vascular resistance while effectively improving systemic hemodynamics. In this regard, the Synergy device may be ideally suited because of its small size and ability to be set at flows as low as 1.5 L/min.

Statement of Conflict of Interest

This work was supported by a grant from the Cardiovascular Medical Research and Education Fund (Philadelphia, PA) awarded to DB. DB is also an employee of CircuLite Inc, the manufacturer of the Synergy micro-pump. The remaining authors have no conflicts of interest to disclose.

References

1. Badesch DB, Tapson VF, McGoon MD, et al. Continuous intravenous epoprostenol for pulmonary hypertension due to the scleroderma spectrum of disease. A randomized, controlled trial. *Ann Intern Med.* 2000;132:425-434.
2. Hoeper MM, Gall H, Seyfarth HJ, et al. Long-term outcome with intravenous iloprost in pulmonary arterial hypertension. *Eur Respir J.* 2009;34:132-137.
3. Lang I, Gomez-Sanchez M, Kneussl M, et al. Efficacy of long-term subcutaneous treprostinil sodium therapy in pulmonary hypertension. *Chest.* 2006;129:1636-1643.
4. Hoeper MM, Schwarze M, Ehlerding S, et al. Long-term treatment of primary pulmonary hypertension with aerosolized iloprost, a prostacyclin analogue. *N Engl J Med.* 2000;342:1866-1870.
5. Voswinckel R, Enke B, Reichenberger F, et al. Favorable effects of inhaled treprostinil in severe pulmonary hypertension: results from randomized controlled pilot studies. *J Am Coll Cardiol.* 2006;48:1672-1681.

6. Rubin LJ, Badesch DB, Barst RJ, et al. Bosentan therapy for pulmonary arterial hypertension. *N Engl J Med.* 2002;346:896-903.
7. Galie N, Ghofrani HA, Torbicki A, et al. Sildenafil citrate therapy for pulmonary arterial hypertension. *N Engl J Med.* 2005;353: 2148-2157.
8. Bogaard HJ, Abe K, Vonk NA, et al. The right ventricle under pressure: cellular and molecular mechanisms of right-heart failure in pulmonary hypertension. *Chest.* 2009;135:794-804.
9. Bogaard HJ, Natarajan R, Henderson SC, et al. Chronic pulmonary artery pressure elevation is insufficient to explain right heart failure. *Circulation.* 2009;120:1951-1960.
10. Haddad F, Skhiri M, Michelakis E. Right ventricular dysfunction in pulmonary hypertension. In: Yuan J, editor. Textbook of Pulmonary Vascular Disease. Springer Science and Business Media; 2011. p. 1313-1332.
11. Price LC, Wort SJ, Finney SJ, et al. Pulmonary vascular and right ventricular dysfunction in adult critical care: current and emerging options for management: a systematic literature review. *Crit Care.* 2010;14:R169.
12. Meyns B, Ector J, Rega F, et al. First human use of partial left ventricular heart support with the CirculiteTM synergyTM micro-pump as a bridge to cardiac transplantation. *Eur Heart J.* 2008;29:2582.
13. Meyns B, Rega F, Ector J, et al. Partial left ventricular support implanted through minimal access surgery as a bridge to cardiac transplant. *J Thorac Cardiovasc Surg.* 2009;137:243-245.
14. Meyns B, Klotz S, Simon A, et al. Proof of concept: hemodynamic response to long-term partial ventricular support with the synergy pocket micro-pump. *J Am Coll Cardiol.* 2009;54:79-86.
15. Rich S, Dodin E, McLaughlin VV. Usefulness of atrial septostomy as a treatment for primary pulmonary hypertension and guidelines for its application. *Am J Cardiol.* 1997;80:369-371.
16. Morley D, Litwak K, Ferber P, et al. Hemodynamic effects of partial ventricular support in chronic heart failure: results of simulation validated with in vivo data. *J Thorac Cardiovasc Surg.* 2007;133:21-28.
17. Grapsa J, Gibbs JS, Cabrita IZ, et al. The association of clinical outcome with right atrial and ventricular remodelling in patients with pulmonary arterial hypertension: study with real-time three-dimensional echocardiography. *Eur Heart J Cardiovasc Imaging.* 2012.
18. Kawut SM, Taichman DB, Archer-Chicko CL, et al. Hemodynamics and survival in patients with pulmonary arterial hypertension related to systemic sclerosis. *Chest.* 2003;123:344-350.
19. Kapur NK, Paruchuri V, Korabathina R, et al. Effects of a percutaneous mechanical circulatory support device for medically refractory right ventricular failure. *J Heart Lung Transplant.* 2011;30:1360-1367.
20. Keogh AM, Mayer E, Benza RL, et al. Interventional and surgical modalities of treatment in pulmonary hypertension. *J Am Coll Cardiol.* 2009;54:S67-S77.
21. Koeken Y, Kuijpers NH, Lumens J, et al. Atrial septostomy benefits severe pulmonary hypertension patients by increase of left ventricular preload reserve. *Am J Physiol Heart Circ Physiol.* 2012;302:H2654-H2662.
22. Gregoric ID, Chandra D, Myers TJ, et al. Extracorporeal membrane oxygenation as a bridge to emergency heart-lung transplantation in a patient with idiopathic pulmonary arterial hypertension. *J Heart Lung Transplant.* 2008;27:466-468.
23. Rajdev S, Benza R, Misra V. Use of Tandem Heart as a temporary hemodynamic support option for severe pulmonary artery hypertension complicated by cardiogenic shock. *J Invasive Cardiol.* 2007;19: E226-E229.
24. Saouti N, Westerhof N, Postmus PE, et al. The arterial load in pulmonary hypertension. *Eur Respir Rev.* 2010;19:197-203.
25. Dickstein ML, Burkhoff D. A theoretic analysis of the effect of pulmonary vasodilation on pulmonary venous pressure: implications for inhaled nitric oxide therapy. *J Heart Lung Transplant.* 1996;15: 715-721.
26. Burkhoff D, Tyberg JV. Why does pulmonary venous pressure rise following the onset of left ventricular dysfunction: a theoretical analysis. *Am J Physiol.* 1993;265:H1819-H1828.
27. Lourenco AP, Fontoura D, Henriques-Coelho T, et al. Current pathophysiological concepts and management of pulmonary hypertension. *Int J Cardiol.* 2012;155:350-361.
28. Correia-Pinto J, Henriques-Coelho T, Roncon-Albuquerque R Jr, et al. Time course and mechanisms of left ventricular systolic and diastolic dysfunction in monocrotaline-induced pulmonary hypertension. *Basic Res Cardiol.* 2009;104:535-545.
29. Xie GY, Lin CS, Preston HM, et al. Assessment of left ventricular diastolic function after single lung transplantation in patients with severe pulmonary hypertension. *Chest.* 1998;114:477-481.
30. Kasner M, Westermann D, Steendijk P, et al. LV dysfunction induced by a non-severe idiopathic pulmonary arterial hypertension. A pressure-volume relationship study. *Am J Respir Crit Care Med.* 2012.
31. Sandoval J, Gaspar J, Pulido T, et al. Graded balloon dilation atrial septostomy in severe primary pulmonary hypertension. A therapeutic alternative for patients nonresponsive to vasodilator treatment. *J Am Coll Cardiol.* 1998;32:297-304.
32. Santamore WP, Burkhoff D. Hemodynamic consequences of ventricular interaction as assessed by model analysis. *Am J Physiol.* 1991;260:H146-H157.
33. Guyton AC, Lindsey AW, Abernathy B, et al. Venous return at various right atrial pressures and the normal venous return curve. *Am J Physiol Heart Circ Physiol.* 1957;189:609-615.
34. Guyton AC, Armstrong GG, Chipley PL. Pressure-volume curves of the arterial and venous systems in live dogs. *Am J Physiol Heart Circ Physiol.* 1956;184:253-258.
35. Klotz S, Meyns B, Simon A, et al. Partial mechanical long-term support with the CircuLite Syndergy pump as bridge-to-transplant in congestive heart failure. *Thorac Cardiovasc Surg.* 2010;58(Suppl 2): S173-S178.
36. Milnor WR. Hemodynamics. Baltimore: Williams and Wilkins; 1982. p. 1.
37. Sagawa K, Maughan WL, Suga H, et al. Cardiac contraction and the pressure-volume relationship. Oxford: Oxford University Press; 1988. p. 1.
38. Alexander J Jr, Sunagawa K, Chang N, et al. Instantaneous pressure-volume relation of the ejecting canine left atrium. *Circ Res.* 1987;61: 209-219.

Appendix

The cardiovascular system was modeled as shown by the electrical analog in Figure A1. The details of this model are provided elsewhere[26,32] and will be discussed here in brief. Ventricular and atrial pumping characteristics were represented by modifications of the time-varying elastance [($E(t)$)] theory of chamber contraction which relates instantaneous ventricular pressure [$P(t)$] to instantaneous ventricular volume [$V(t)$]. For each chamber:

$$P(t) = P_{ed}(V) + e(t)[P_{es}(V) - P_{ed}(V)]$$

In which:

$$P_{ed}(V) = \beta\left(e^{\alpha(V-Vo)} - 1\right)$$

$$P_{es}(V) = E_{es}(V - V_o)$$

and

$$e(t) = \begin{cases} \frac{1}{2}\{\sin[(\pi / T_{max})t - \pi/2] + 1\} & 0 < t \le 3/2T_{max} \\ \frac{1}{2}e^{-(t-3T_{max}/2)/\tau} & t > 3/2T_{max} \end{cases}$$

where $P_{ed}(V)$ is end-diastolic pressure as a function of volume, $P_{es}(V)$ is end-systolic pressure as a function of volume, E_{es} is end-systolic elastance, V_o is the volume axis intercept of the end-systolic pressure-volume relationship (ESPVR), α and β are parameters of the end-diastolic pressure-volume relationship (EDPVR), T_{max} is the point of maximal chamber elastance, τ is the time constant of relaxation and t is the time during the cardiac cycle.

The systemic and pulmonary circuits are each modeled by lumped venous and arterial capacitances (C_v and C_a, respectively), a proximal resistance (R_c, also commonly called *characteristic impedance*) which relates to the stiffness of the proximal aorta or pulmonary artery, a lumped arterial resistance (R_a), and a resistance to return of blood from the venous capacitance to the heart (R_v, which is similar, though not identical, to Guyton's resistance to venous return[33]). The heart valves permit flow in only one direction through the circuit. Tricuspid regurgitation (TR) was introduced by adding a second diode in the opposite direction with a serial resistance that could be adjusted to set the degree of tricuspid regurgitation.

The total blood volume (V_{tot}) contained within each of the capacitive compartments is divided functionally into two pools: the *unstressed* blood volume (Vol_{unstr}) and the *stressed* blood volume (Vol_{str}). Vol_{unstr} is defined as the maximum volume of blood that can be placed within a vascular compartment without raising its pressure above 0 mmHg. The blood volume within the vascular compartment in excess of Vol_{unstr} is Vol_{str}, so that $V_{tot} = V_{unstr} + V_{str}$. The unstressed volume of the entire vascular system is equal to the sum of Vol_{unstr} of all the capacitive compartments; similarly, the total body stressed volume equals the sum of Vol_{str} for all compartments.[34] The pressure within the compartment rises linearly with Vol_{str} in relation to the compliance (C): $P = Vol_{str}/C$.

The RVAD was modeled as a continuous flow pump with approximately linear pressure-flow characteristics that varied with pump speed as shown in Figure A2. These data were obtained from a real Synergy™ System (including inflow and outflow grafts) interfaced with a mock circulation filled with a water-glycerol solution (viscosity 3.6 cp). This pump is currently in clinical trials as a left ventricular assist device to provide partial circulatory support to patients with INTERMACS 4, 5 and 6 heart failure.[14,35] As illustrated, such a pump can generate flows up to 4.25 L/min with its impeller spinning at 28,000 rpm (pressure head between 100 and 150 mmHg). As indicated in Figure A1, it could be specified during the simulation whether the RVAD withdrew blood from the right atrium or from the right ventricle. In either case, the blood was pumped to the proximal portion of the arterial system.

The normal value of each parameter of the model was set to be appropriate for a 70–75 kg man (body surface area 1.9 m^2). These values, adapted from values in the literature[32,36–38] are listed in Table A1. Values used to simulate patients with different degrees of PAH are summarized in the main text, Table 2.

Finally, atrial septostomy was modeled by a connection between right and left atria through which flow was determined by the equation governing flow through an orifice:

$$\text{Flow} = K.\text{Area}.\sqrt{\Delta P}$$

Where A is the area (in cm^2), ΔP is the pressure gradient across the orifice (in mmHg) and $K = 2.66$.

Table A1
Normal parameter values.

Parameter group/name	Symbol	Units	Values			
Common parameters						
Heart rate	HR	min^{-1}	70			
AV delay	AVD	msec	160			
Total blood volume	BV_{tot}	mL	5000			
Stressed blood volume	BV_{stress}	mL	950			
Unstressed blood volume	$BV_{unstress}$	mL	4050			
Heart			RA	RV	LA	LV
End-systolic elastance	E_{es}	mmHg/mL	0.45	0.61	0.45	3
Volume axis intercept	V_o	mL	10	5	10	5
	B	mmHg	0.44	0.35	0.44	1.3

Table A1 (*continued*)

Parameter group/name	Symbol	Units	Values			
Scaling factor for EDPVR						
Exponent for EDPVR	α	mL^{-1}	0.049	0.04	0.049	0.027
Time to end-systole	T_{max}	msec	125	200	125	200
Time constant of relaxation	T	msec	25	30	25	30
AV valve resistance	R_{av}	mmHg.s/mL	0.0025		0.0025	
Circulation			Pulmonary	Systemic		
Characteristic impedance	R_c	mmHg.s/mL	0.03	0.04		
Arterial resistance	R_a	mmHg.s/mL	0.03	1.1		
Venous Resistance	R_v	mmHg.s/mL	0.025	0.025		
Arterial compliance	C_a	mL/mmHg	13	1.5		
Venous compliance	C_v	mL/mmHg	8	70		

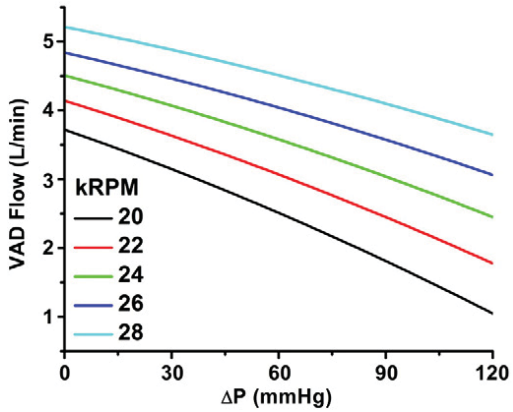

Fig A2. Pressure-flow characteristics of the RVAD.

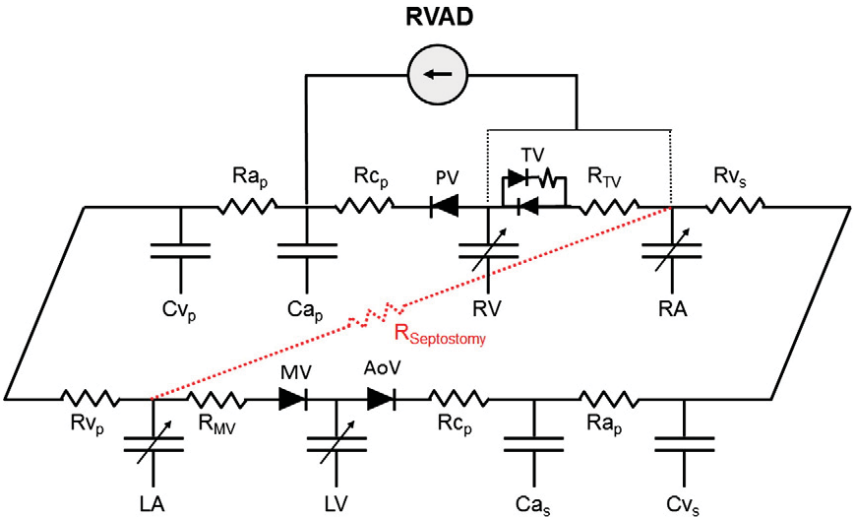

Fig A1. Electrical analog for modeling the cardiovascular system.